Development 140, 2354-2364 (2013) doi:10.1242/dev.088427

A novel chemical screening strategy in zebrafish identifies common pathways in embryogenesis and rhabdomyosarcoma development

Xiuning Le[1], Emily K. Pugach[1], Simone Hettmer[2], Narie Y. Storer[1], Jianing Liu[2], Airon A. Wills[3], Antony DiBiase[1], Eleanor Y. Chen[4], Myron S. Ignatius[4], Kenneth D. Poss[3], Amy J. Wagers[2], David M. Langenau[4] and Leonard I. Zon[1,*]

SUMMARY

The zebrafish is a powerful genetic model that has only recently been used to dissect developmental pathways involved in oncogenesis. We hypothesized that operative pathways during embryogenesis would also be used for oncogenesis. In an effort to define RAS target genes during embryogenesis, gene expression was evaluated in *Tg(hsp70-HRAS^{G12V})* zebrafish embryos subjected to heat shock. *dusp6* was activated by RAS, and this was used as the basis for a chemical genetic screen to identify small molecules that interfere with RAS signaling during embryogenesis. A *KRAS^{G12D}*-induced zebrafish embryonal rhabdomyosarcoma was then used to assess the therapeutic effects of the small molecules. Two of these inhibitors, PD98059 and TPCK, had anti-tumor activity as single agents in both zebrafish embryonal rhabdomyosarcoma and a human cell line of rhabdomyosarcoma that harbored activated mutations in *NRAS*. PD98059 inhibited MEK1 whereas TPCK suppressed S6K1 activity; however, the combined treatment completely suppressed eIF4B phosphorylation and decreased translation initiation. Our work demonstrates that the activated pathways in RAS induction during embryogenesis are also important in oncogenesis and that inhibition of these pathways suppresses tumor growth.

KEY WORDS: RAS, Embryogenesis, Rhabdomyosarcoma, Translational control, Zebrafish

INTRODUCTION

The zebrafish was first established as a powerful vertebrate model organism for large-scale developmental genetic screens (Gaiano et al., 1996; Haffter et al., 1996). Because of the ease and low cost of raising large numbers of fish, and the highly conserved genetic and biochemical pathways between zebrafish and mammals, the zebrafish has also been utilized for chemical screens *in vivo* (North et al., 2007). In the last decade, a variety of zebrafish cancer models have been developed ranging in complexity from carcinogen-induced tumors in wild-type fish to transgenic zebrafish models of specific human oncogenes (Goessling et al., 2007). For example, a *rag2-KRAS^{G12D}*-induced embryonal rhabdomyosarcoma (ERMS) revealed that zebrafish and human ERMS share two conserved gene signatures, one of which is associated with tissue-restricted gene expression in rhabdomyosarcoma and a second that comprises a RAS-induced gene signature (Langenau et al., 2007). These zebrafish cancer models share similar histopathological features and molecular pathways to human disease, and respond to drugs in a similar manner as humans, and thus can be implemented in different steps of novel anti-cancer agent development.

[1]Stem Cell Program and Division of Hematology/Oncology, Children's Hospital and Dana Farber Cancer Institute, Howard Hughes Medical Institute, Harvard Stem Cell Institute, Harvard Medical School, Boston, MA 02115, USA.[2]Howard Hughes Medical Institute, Department of Stem Cell and Regenerative Biology, Harvard University, Harvard Stem Cell Institute, Joslin Diabetes Center, Boston, MA 02115, USA. [3]Department of Cell Biology, Howard Hughes Medical Institute, Duke University Medical Center, Durham, NC 27710, USA. [4]Molecular Pathology Unit, Department of Pathology, Massachusetts General Hospital, Charlestown, MA 02129 and Harvard Stem Cell Institute, Boston, MA 02114, USA.

*Author for correspondence (zon@enders.tch.harvard.edu)

Accepted 25 March 2013

The RAS pathway is a key developmental pathway during embryogenesis. In developing zebrafish embryos, the FGF/RAS pathway plays an antagonistic role with the BMP pathway in dorsal-ventral patterning (Schier, 2001). The RAS genes encode a family of GTPases, which function as binary molecular switches that transduce extracellular growth factor signaling to control intracellular pathways to modulate diverse cellular responses including proliferation, differentiation and survival (Malumbres and Barbacid, 2003). RAS activates various mitogen-activated protein kinases (MAPKs), including extracellular signal-regulated kinase (ERK). Activated ERK regulates diverse gene expression programs through transcription factors and the translation machinery (McCubrey et al., 2007). RAS also binds directly to PI3K and initiates the AKT/mTOR signal transduction cascade (Rodriguez-Viciana et al., 1994). The best-characterized downstream targets of mTOR are ribosomal protein S6 kinase 1 (S6K1; also known as p70S6K or RPS6KB1) and eukaryotic translation initiation factor 4E-binding protein 1 (EIF4EBP1), both of which are crucial to the regulation of protein synthesis (Anjum and Blenis, 2008). Thus, RAS signaling regulates translation through diverse mechanisms.

RAS family members are the most commonly mutated oncogenes in human cancers (Bos, 1989). Point mutations in RAS genes constitutively activate the above-mentioned pathways to drive cell overproliferation. Given the prevalence of RAS signaling activation in human cancers, a significant effort has been dedicated to developing both inhibitors of RAS activation and its downstream signaling pathways, such as MEK and mTOR (Easton and Houghton, 2006; Sebolt-Leopold et al., 1999). Although experimental agents are under development, there are as yet no clinically available drugs directly targeting the RAS pathway. Understanding RAS signaling in tumors and targeting RAS pathways to treat tumors remain a challenge.

In the last decade, multiple zebrafish cancer models have been generated with RAS mutations, including *KRAS*-induced myeloproliferative disease, rhabdomyosarcoma, colon adenoma and hepatocellular carcinoma, and *NRAS*-induced melanoma (Dovey et al., 2009; Langenau et al., 2007; Le et al., 2007). The short time to tumor onset and ease of fluorescent labeling of tumors, together with the feasibility of creating large numbers of animals, make zebrafish an advantageous model for chemical genetic studies to aid our understanding of RAS oncology.

Here, a two-step screening approach was undertaken to examine whether RAS activation in zebrafish embryogenesis illuminates possible mechanisms operative in tumors: first, we used zebrafish embryos to dissect RAS pathways and identified anti-RAS chemicals *in vivo*; second, we evaluated the therapeutic value of each hit in a zebrafish model of *KRAS*-induced ERMS. Two compounds (PD98059 and TPCK) demonstrated efficacy in suppressing fish tumor growth. Combined treatment resulted in enhanced therapeutic efficacy. Finally, we investigated the mechanism of combined treatment with PD98059 and TPCK, and revealed the importance of suppression of translation initiation in RAS-activated tumor cells. Our studies utilized common pathways activated by oncogenic RAS during embryogenesis and rhabdomyosarcoma development, and established that developing zebrafish embryos can provide a productive platform for the identification of anticancer agents.

MATERIALS AND METHODS

Animals and stable transgenic lines

Zebrafish (*Danio rerio*) were maintained in accordance with Animal Research Guidelines at Children's Hospital Boston. The *Tg(hsp70-HRAS^{G12V})* stable transgenic line (http://zfin.org/action/genotype/genotype-detail?zdbID=ZDB-GENO-100723-7) was first described by Lee et al. (Lee et al., 2009). The *Tg(dusp6-d2EGFP)* transgenic line (http://zfin.org/action/fish/fish-detail/ZDB-GENO-071017-5,ZDB-GENOX-110131-12,ZDB-GENOX-120807-2) was generously provided by Professor Michael Tang (University of Pittsburgh).

Microarray analysis

Heterogeneous *Tg(hsp70-HRAS^{G12V})* embryos were obtained by mating male homozygous transgenic fish to wild-type females. They were raised to 24 hours post-fertilization (hpf) and received heat shock at 37°C in a waterbath for 1 hour, and were then kept at 28.5°C until 30 hpf for RNA extraction by Trizol reagent (Invitrogen). Wild-type embryos (AB strain) receiving the same heat shock treatment were used as controls. Each microarray sample was prepared by pooling 50 embryos. Biological duplicates were obtained in both transgenic groups and controls. NimbleGen array chips were used. The probe-level data were normalized and translated to gene-level with custom Python scripts, then analyzed with Goldenspike (http://www2.ccr.buffalo.edu/halfon/spike/). The R Goldenspike package background-corrects, normalizes, multiple-tests, and computes the sample statistics per chip. The annotation of the zebrafish probe sets was completed using the Zon Laboratory/Children's Hospital Zebrafish Gene Transcription Collection (ZGTC; http://zfrhmaps.tch.harvard.edu/zgmap/ZGTC.htm). The dataset was deposited at Gene Expression Omnibus under accession number GSE 44364.

Quantitative RT-PCR

RNA was isolated from whole zebrafish embryos at 30 hpf using RNAlater and RNeasy Kits (Qiagen). RNA was reverse transcribed using the High Capacity cDNA Reverse Transcription Kit (Applied Biosystems), and quantitative PCR was performed using SYBR Green (Invitrogen). PCR primers are described in supplementary material Table S1.

Chemical library

A collection of 2896 compounds was screened in zebrafish embryos for suppressors of oncogenic RAS. Among these, 2460 compounds were from ICCB-Longwood Harvard Medical School, including: Biomol ICCB known bioactives [480 compounds, 5 mg/ml (~13 mM) as stock, 33.3 μg/ml final concentration], NINDS (1040 compounds, 10 mM as stock, 66 μM final concentration), Prestwick (1120 compounds, 2 mg/ml as stock, 13.3 μM final concentration). 256 compounds were from HSCI/CHB hESC Core (1-5 mg/ml as stock, 6.7-33.3 μg/ml final concentration). Each chemical was screened at a single concentration (1/150 of stock concentration).

Embryonic RAS screen

A chemical screen (see Fig. 2A) was designed using heat shock-inducible *Tg(hsp70-HRAS^{G12V})* embryos. Pathway activation was read out using *dusp6* mRNA expression. Heterozygous *Tg(hsp70-HRAS^{G12V})* embryos were raised at 28°C until 22 hpf and then transferred to a 48-well tissue culture plate (8-15 embryos per well), where each well contained a test chemical dissolved in embryo water. After 2 hours of chemical treatment, heat shock was applied by incubating the 48-well plates at 37°C in a water bath for 1 hour. Then, 24-hpf embryos were returned to a 28°C incubator and fixed at 30 hpf. *dusp6* expression levels were evaluated by *in situ* hybridization and classified as: (1) complete suppression of *dusp6* in all embryos; (2) partial/complete suppression with more than two-thirds of embryos having suppression of *dusp6* expression; (3) no effect; and (4) enhancement of *dusp6* expression in more than two-thirds of embryos. In each 48-well plate, two wells received no chemical treatment and two wells did not receive heat shock.

Therapeutic evaluation using a zebrafish model of RAS-induced ERMS

One-cell stage AB strain zebrafish were injected with *rag2-KRAS^{G12D}* and *rag2-DsRed*. Injected animals were screened under a fluorescence microscope at 7 days post-fertilization (dpf) to identify DsRed-positive tumor-bearing fish. All the tumor-bearing fish were numbered, raised in isolated tanks, and randomized into two groups. One group received chemical treatment at the maximum tolerated dose (MTD) while the other received vehicle treatment. MTD was determined by incubating 7-dpf wild-type larval fish in the compound for 5 days and was experimentally defined as the dose at which 75% of fish survived treatment. Each group received two consecutive days of treatment, at day 7 and day 8, of either compound or vehicle control. At 9 dpf, animals were fed with paramecium and fresh water added to the wells to allow recovery and growth of fish over this time. From 10-11 dpf, animals were again bathed in compound or DMSO vehicle. At day 12, animals received feeding and fresh water as at day 9. At days 7, 10 and 13, animals were photographed using a defined exposure time, magnification and gain. Tumor size was measured by quantifying the total number of pixels within the fluorescent area. The relative tumor growth was defined as total pixel numbers at day 10 or day 13 normalized by the total pixel number at day 7 (see Fig. 3B-D). Researchers were blinded as to which animals received treatment or control vehicle until completion of imaging on day 13.

Human cell culture, shRNA knockdown and reporter assay

The human rhabdomyosarcoma RD cell line and the mouse embryonic fibroblast (MEF) cell line were generously provided by Professor Amy Wagers (Harvard Medical School). Cells were maintained in DMEM (Roche) with 10% FBS and 1% penicillin/streptomycin. Cells were plated and proliferation was measured (by MTT Assay Kit, Cayman Chemical) as described in the results. Apoptotic levels were measured by TdT assay (TiterTACS Kit, Trevigen).

For S6K1 knockdown, lentiviral vectors were purchased from Open Biosystems (TRCN0000003158 and TRCN0000003159), and lentiviral particles were produced by cotransfection of HEK 293T cells with pLKO.1 constructs and packaging plasmids pMD.G and pCMVR8.91 (A.J.W. lab.). Transfections were carried out with FuGENE 6 (Promega), and virus was harvested 48 hours after transfection and frozen. To test the efficacy of shS6K1, RD cells were incubated with lentiviral supernatants in the presence of 8 mg/ml Polybrene (American Bioanalytical) for 24 hours, and infected cells were selected with 10 mg/ml puromycin. After 48 hours of selection, cells were evaluated by MTT assay on day 3, 5 and 7 for proliferation. To test the synergistic effect of S6K1 with PD98059, RD cells

were incubated with lentiviral supernatant (TRCN0000003158) (shS6K1-58) in the presence of 8 mg/ml Polybrene, and infected cells were selected with 10 mg/ml puromycin. After 48 hours of selection, cells were washed and cultured in medium containing chemicals or vehicle controls. Medium containing chemicals or vehicle controls was changed on day 7 and day 9 for continuous chemical exposure and selection. Cell proliferation was evaluated by MTT assay on day 5, 7 and 9.

The bicistronic reporter SV40-Renilla-IRES-Firefly was provided by Dr John Blenis (Harvard Medical School). The plasmid was transfected into RD cell lines using FuGENE 6 (Promega) and kept in complete medium. At 24 hours post-transfection, cells were starved for 12 hours, and then treated with chemicals or controls. Thirty minutes after chemical exposure, serum (20%) was added to cells to stimulate translation. Luciferase activities were measured 4 hours after serum stimulation (Dual-Luciferase Assay System, Promega), and the Renilla/firefly luciferase light unit ratio was calculated.

Western blotting

Anti-phospho-Erk1/2, anti-total Erk1/2, anti-phospho-AKT (Ser473) and anti-phospho-S6 ribosomal protein (Ser240/244) were purchased from Cell Signaling. Anti-actin antibody was from MP Biomedicals. The use of secondary antibodies, dilution of primary antibodies and blocking were performed according to the manufacturer's recommendations. Zebrafish embryos were collected and manually homogenized in 1× SDS sample buffer and subjected to SDS-PAGE followed by blotting onto nitrocellulose membrane. RD cells were harvested in 1× sample buffer and subjected to SDS-PAGE followed by blotting onto nitrocellulose membrane. ECL detection reagents were used (GE Healthcare).

RESULTS

Establishing a chemical screen platform using inducible RAS zebrafish embryos to dissect tumorigenesis pathways

The activation of RAS during embryogenesis may recapitulate the activation of its pathways during tumorigenesis. We sought to evaluate the effects of increased RAS activity on embryos. Injection of oncogenic *RAS* mRNA into zebrafish results in early embryonic death. To bypass the RAS-induced lethality, we used an inducible transgenic zebrafish line that expresses the human $HRAS^{G12V}$ gene under the heat shock promoter, *Tg(hsp70-*$HRAS^{G12V}$*)* (Lee et al., 2009), and induced RAS expression after gastrulation.

A microarray analysis was performed by comparing the transcription profiles of *Tg(hsp70-*$HRAS^{G12V}$*)* and wild-type embryos subjected to heat shock. Both groups of embryos received heat shock at 37°C for 1 hour at 24 hpf, and were kept at 28.5°C until 30 hpf for RNA extraction. Three different fold change cut-offs were utilized in defining the upregulated gene lists to verify that differences were reproducibly related to RAS activation and not due to arbitrary assignment of gene lists. Using a false discovery rate (FDR) of zero and log fold change cut-offs greater than 1, 0.7 and 0.5 (with the correlating absolute fold change greater than 2, 1.6245 and 1.4142), three gene lists compassing 2423, 3540 and 4129 genes were defined as upregulated (supplementary material Table S2; downregulated genes are listed in Table S3). Ingenuity pathway analysis (IPA) was performed using the three lists. In all three analyses, 'cancer' was the top 'diseases and disorders', with 'developmental disorder' and 'organismal injury and abnormalities' as second and third 'diseases and disorders' (Fig. 1A), strongly suggesting that transient induction of oncogenic RAS in embryos activates major pathways in oncogenesis.

To identify a downstream gene readout for a chemical screen, we examined a set of 17 genes that were found to be upregulated in zebrafish rhabdomyosarcomas (Langenau et al., 2007). These 17 genes (Table 1) included 12 from a signature that was defined as commonly upregulated genes in zebrafish ERMS, human ERMS, human pancreatic cancer and RAS-infected human mammary epithelial cells (HMECs). The remaining five were selected from genes that were upregulated in one or two RAS-related conditions (Fig. 1B). Among the 17 genes, seven were upregulated as assessed by microarray analysis in whole embryos. Four genes, namely *fgf3*, *sat*, *dusp4* and *dusp6*, were confirmed to be upregulated by RT-PCR (Table 1; Fig. 1C).

Among these, *dusp6* (*mkp3*), a known target of the FGF signaling pathway and a negative regulator of Erk1/2 (Mapk3/1) (Ekerot et al., 2008), was robustly upregulated in 100% of the heat shocked heterozygous *Tg(hsp70-*$HRAS^{G12V}$*)* embryos, demonstrating strong staining by *in situ* hybridization (ISH). Such activation was also confirmed in the *Tg(dusp6-d2EGFP)* reporter line (supplementary material Fig. S1). Furthermore, *dusp6* was concordantly upregulated in *rag2-*$KRAS^{G12D}$-induced zebrafish ERMS as detected by ISH on the tumor sections, confirming *dusp6* as a target of oncogenic RAS in tumors (supplementary material Fig. S2). *dusp6* was therefore chosen as the readout of the chemical screen because of its robust activation by RAS in early larval development and its biological relevance in RAS tumorigenesis.

Several pathway-specific chemical inhibitors were next tested to demonstrate that RAS activation could be suppressed in a pathway-specific manner in this inducible embryonic system. The effects of a RAS activation inhibitor (Lovastatin), MAPK pathway inhibitors (Raf1 inhibitor or PD98059) and a PI3K inhibitor (Wortmannin) were tested in embryos. We first utilized *erm* (*etv5b* – Zebrafish Information Network), a previously established target in heat shocked *Tg(hsp70-*$HRAS^{G12V}$*)* embryos [see supplementary figure 2 in Lee et al. (Lee et al., 2009)]. Erm is one of the Ets transcription factors, and a known transcription target of the FGF/MAPK pathway (Janknecht et al., 1996; Roehl and Nüsslein-Volhard, 2001) but not the PI3K/AKT pathway. Embryos were assessed for levels of *erm* by ISH as well as RT-PCR (Fig. 1D,E). As predicted, the level of *erm* was suppressed by RAS or MAPK inhibitors, but not by Wortmannin. By contrast, *dusp6* (Fig. 1E) expression was suppressed by RAS and MAPK inhibitors, but also partially suppressed by Wortmannin, which is consistent with previous observations in chick limb buds that *Dusp6* is suppressed by PI3K inhibitor (Kawakami et al., 2003). Expression of *dusp4* and *sat* was regulated in a similar manner to *dusp6* (supplementary material Fig. S3). The differential responses of genes to pathway-specific inhibitors confirmed that *Tg(hsp70-*$HRAS^{G12V}$*)* transgenic larvae could be used in a chemical screen to uncover drugs that inhibit RAS and its downstream targets.

Identification of suppressors of RAS signaling through a zebrafish embryonic chemical screen

The chemical screen was further optimized by utilizing RT-PCR and *Tg(dusp6-d2EGFP)* reporter line transgenic fish to determine peak expression of *dusp6*. Both approaches demonstrated that, at 6 hours post-heat shock, embryos exhibited peak expression of *dusp6* (Fig. 2A, dashed line; supplementary material Figs S1, S4). Therefore, 6 hours post-heat shock was chosen as the time for readout of RAS activity.

A collection of 2896 bioactive small molecules was screened for compounds that suppress *dusp6* expression following heat shock in *Tg(hsp70-*$HRAS^{G12V}$*)* embryos (Fig. 2; also see Materials and methods). This collection includes many classes of well-characterized compounds such as ion channel blockers, nuclear receptor ligands, protease inhibitors, gene regulation agents and lipid biosynthesis inhibitors, and covers more than 46% of Food and Drug Administration-approved drugs. Each compound was

A

Top Networks

ID	Associated Network Functions	Score
1	Cell-To-Cell Signaling and Interaction, Nervous System Development and Function, Infectious Disease	39
2	Cellular Growth and Proliferation, Cellular Development, Embryonic Development	37
3	Cancer, Endocrine System Disorders, Gastrointestinal Disease	35
4	Nervous System Development and Function, Tissue Morphology, Developmental Disorder	34
5	Cell Morphology, Cellular Assembly and Organization, Cellular Development	31

Top Bio Functions

Diseases and Disorders

Name	p-value	# Molecules
Cancer	5.86E-18 - 1.37E-05	570
Developmental Disorder	1.11E-16 - 1.04E-05	240
Organismal Injury and Abnormalities	2.77E-16 - 1.82E-05	181
Infectious Disease	2.72E-10 - 1.22E-05	225
Neurological Disease	6.68E-10 - 1.28E-05	299

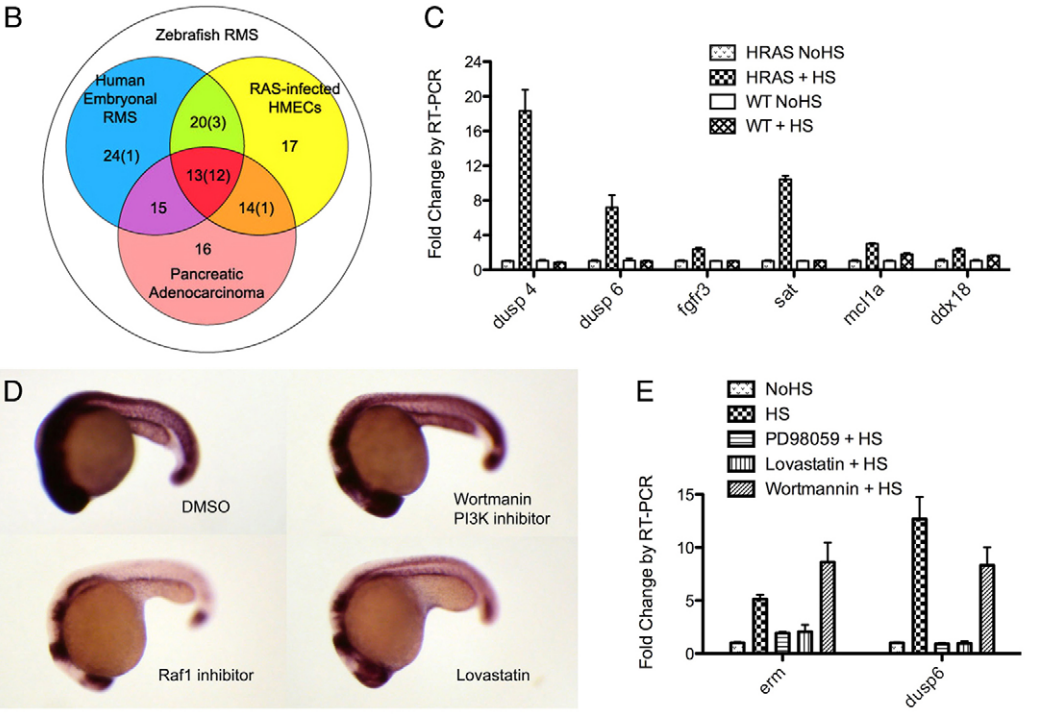

Fig. 1. Transient RAS action in *Tg(hsp70-HRAS^{G12V})* zebrafish embryos resembles pathway activation during tumorigenesis. (**A**) Ingenuity pathway analysis output for the upregulated gene set identified on comparing *Tg(hsp70-HRAS^{G12V})* embryos to wild-type zebrafish embryos following heat shock (log fold change >0.5 for top network and >0.7 for top diseases and disorders). (**B**) RAS signature gene list, defined as commonly upregulated genes in zebrafish RMS (white circle), human embryonal RMS (blue circle), human pancreatic adenocarcinoma (red circle) and RAS-infected HMECs (yellow circle). The total number of genes is shown, with the number tested in the 17-gene list in parentheses [adapted from Langenau et al. (Langenau et al., 2007)]. (**C**) RT-PCR analysis of six of the RAS signature genes in *Tg(hsp70-HRAS^{G12V})* and wild-type embryos with and without heat shock. $P<0.05$ for each gene shown, HRAS+HS compared with other conditions. (**D**) ISH of *erm*. Transgenic embryos were incubated with various chemicals from 16 hpf, heat shocked at 18-19 hpf, and fixed at 24 hpf. DMSO, vehicle control. (**E**) RT-PCR analysis of *erm* and *dusp6* expression levels in response to pathway-specific chemical inhibitors. Error bars indicate s.e.m. HS, heat shock; NoHS, no heat shock.

screened at a single concentration with 5-10 embryos. Thirty-one of the 2896 compounds screened demonstrated complete suppression of *dusp6* expression and another 67 exhibited partial suppression (Table 2). The 31 compounds with the most potent suppression were purchased and individually retested using the same experimental conditions and concentration. Twenty-five (80.6%) of the 31 retested chemicals were validated to have potent suppressive effects on *dusp6*, indicating that the primary screen could robustly identify suppressors of the RAS signaling pathway.

Heat shock was applied to *Tg(hsp70-HRAS^{G12V})* embryos after 2 hours of chemical exposure; thus, our experimental design would be likely to identify drugs that suppress both RAS activity and heat shock responses. To select drugs that specifically affect RAS pathway activation, *Tg(hsp70-Cre)* fish were assessed for *Cre* expression following heat shock and subsequent drug treatment (Le et al., 2007). Chemicals that suppressed *Cre* mRNA expression were eliminated from further study, as these compounds were likely to regulate *hsp70* promoter expression and/or the heat shock response rather that RAS activity (supplementary material Fig. S5). Using this approach, 18 compounds were confirmed as RAS pathway inhibitors (supplementary material Table S4).

Identification of chemical inhibitors of RAS-induced embryonal rhabdomyosarcoma

To evaluate the effects of the 18 RAS signaling pathway inhibitors in cancer, each chemical was tested as a single agent for suppressing

Table 1. The 17 genes tested to identify a robust readout for the chemical screen

Gene	Gene in maximally contributing group	RT-PCR (whole embryos)	Microarray (whole embryos)	NimbleGen ID	Fold change in microarray	q value (FDR)
csf1r	hERMS	–	Up	NM_131672	3.336	0
lrrfip1	hERMS; RAS-infected HMECs	–	Up	ZV700S00003373	2.416	0
dusp4	hERMS; RAS-infected HMECs	Up	Up	ZV700S00006581	2.640	0
				OTTDART00000029337	2.081	0
dusp6	hERMS; RAS-infected HMECs	Up	Up	OTTDART00000026849	1.708	0
				AY278203.1	1.667	0
gbp1	RAS-infected HMECs; pancreas	–	–	–	–	–
arpc1b	hERMS; RAS-infected HMECs; pancreas	–	–	–	–	–
calr	hERMS; RAS-infected HMECs; pancreas	–	–	–	–	–
ctsl	hERMS; RAS-infected HMECs; pancreas	–	–	–	–	–
ddx18	hERMS; RAS-infected HMECs; pancreas	Up	–	–	–	–
fgfr3	hERMS; RAS-infected HMECs; pancreas	Up	Up	OTTDART00000026660	1.775	0
mcl1	hERMS; RAS-infected HMECs; pancreas	Up	–	–	–	–
msn	hERMS; RAS-infected HMECs; pancreas	–	Up	OTTDART00000004950	1.520	0
pdia3	hERMS; RAS-infected HMECs; pancreas	–	–	–	–	–
psmb2	hERMS; RAS-infected HMECs; pancreas	–	–	–	–	–
sat	hERMS; RAS-infected HMECs; pancreas	Up	Up	ZV700S00002566	2.490	0
snrpd3	hERMS; RAS-infected HMECs; pancreas	–	–	–	–	0
ssb	hERMS; RAS-infected HMECs; pancreas	–	–	–	–	–

hERMS, human embryonal rhabdomyosarcoma; HMECs, human mammary epithelial cells.

zebrafish *KRAS*^{G12D}-induced RMS using a randomized trial design. Co-injection of *rag2-KRAS*^{G12D} and *rag2-DsRed* DNA leads to externally visible zebrafish ERMS by 10 days (Langenau et al., 2008). As early as 7 dpf, tumor-bearing fish can be identified by visualizing DsRed fluorescence in muscle fibers, with 100% of DsRed-positive animals developing ERMS (n=11). ERMS growth can be followed within individual animals by serial imaging over several days based on the fluorescent tumor area. The therapeutic effect of each compound can be quantified by determining relative tumor growth as compared with that in non-treated animals (Fig. 3A-F; see also Materials and methods).

Two compounds significantly delayed tumor growth at their maximum tolerated dose (MTD). The MEK inhibitor PD98059 (supplementary material Fig. S6A; MTD 15.2 μM) inhibited relative tumor growth (1.259±0.171, n=13 at day 10; 1.373±0.285, n=8 at day 13) as compared with vehicle-treated sibling fish (1.778±0.906, n=10 at day 10; 2.034±1.621, n=10 at day 13; P<0.05, ANOVA; Fig. 3G). The chymotrypsin-like serine protease inhibitor tosyl

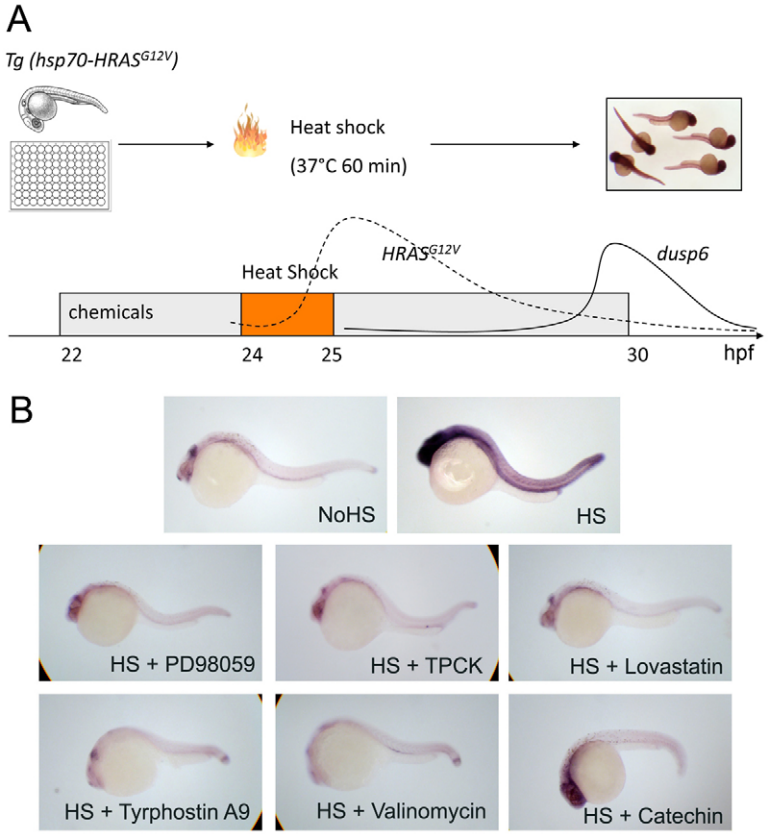

Fig. 2. A small-molecule screen in *Tg(hsp70- HRAS*^{G12V}*)* zebrafish embryos. (**A**) Scheme of the chemical screen. Heterozygous *Tg(hsp70-HRAS*^{G12V}*)* embryos were placed in a 48-well plate for chemical treatment starting at 22 hpf and heat shocked from 24-25 hpf in a 37°C waterbath to activate RAS signaling (dashed line). At 30 hpf, embryos were fixed and the *dusp6* expression level was evaluated by ISH. The solid line represents the dynamic changes in *dusp6* RNA level, as confirmed by RT-PCR; the dashed line represents the predicted activation of RAS based on *hsp70* promoter dynamics (Le et al., 2007). (**B**) ISH of *dusp6* on embryos treated with PD98059, TPCK, Lovastatin, Tyrphostin A9, Valinomycin and Catechin.

Table 2. Screening of 2896 compounds for effect on *dusp6* expression

Effect	Number of compounds	Percentage
Severe toxicity	78	2.69
Complete suppression	31	1.07
Partial suppression	67	2.31
No effect	2703	93.3
Enhancement	17	0.59

phenylalanyl chloromethyl ketone (TPCK; supplementary material Fig. S6B; MTD 0.3 μM) also inhibited relative tumor growth as a single agent (1.056±0.163, n=15 at day 10; 1.058±0.293, n=6 at day 13) as compared with vehicle-treated sibling fish (P<0.05, ANOVA; Fig. 3H). The gross morphology of the fish was not affected by chemical treatment. Their swimming and eating behaviors were also normal. To ensure that chemical effects were specific to tumors and did not affect the growth of the entire fish, the overall length of each fish was recorded under brightfield illumination at 7, 10 and 13 dpf. Neither TPCK nor PD98059 significantly altered overall fish growth at the MTD when compared with vehicle-treated fish (supplementary material Fig. S7A,B). No statistically significant difference in survival was detected among chemical-treated groups versus controls (P=0.53, ANOVA). The impaired survival in the treatment trials was likely to be due to reduced feeding, repeated anesthesia for imaging, and mechanical manipulation during larval development.

Taken together, we have developed a two-step screening system for the oncogenic RAS pathway: we first identified 18 chemical suppressors of RAS signaling pathways during zebrafish embryogenesis, and then found that two of them – PD98059 and TPCK – have effects in suppressing tumor growth in a genetically engineered zebrafish model of ERMS.

PD98059 and TPCK suppress different downstream RAS signaling targets

We measured the activity levels of selected RAS targets to understand how the two hits affect RAS signaling pathways. PD98059 is a known MEK1 (MAP2K1) inhibitor and has been previously shown to inhibit MEK activity in zebrafish (Pozios et al., 2001). PD98059 suppressed *dusp6* expression in zebrafish embryos in a dose-dependent manner (supplementary material Fig. S8). Western blot analysis (Fig. 4) showed that PD98059 (18.7 μM) suppressed phospho (p-) Erk1/2 levels in zebrafish embryos, but not levels of p-Akt or p-p38 (Mapk14 – Zebrafish Information Network) (data not shown), demonstrating that PD98059 indeed inhibits the MAPK pathway in zebrafish. TPCK was originally designed as a chymotrypsin-like serine protease inhibitor; however, it has subsequently been shown to be a potent inhibitor of S6K1. In the *Tg(hsp70-HRAS^{G12V})* embryos, TPCK suppressed *dusp6* expression in a dose-dependent manner (supplementary material Fig. S8). Western analysis indicated that the levels of p-Rps6, which is a target of S6k1, were greatly suppressed in zebrafish embryos treated with TPCK (1 μM), indicating that TPCK suppressed S6k1 activity in zebrafish embryos. TPCK did not alter the levels of p-Erk1/2 or p-Akt in zebrafish (Fig. 4). These results suggest that PD98059 suppresses the MAPK pathway of RAS signaling, whereas TPCK specifically suppresses

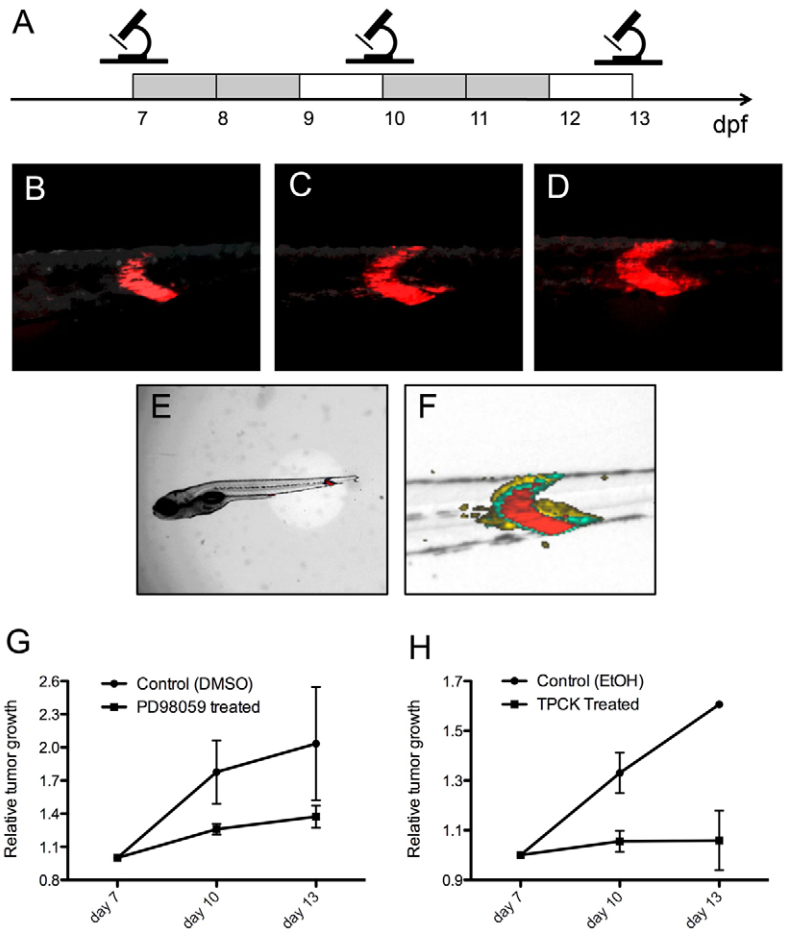

Fig. 3. PD98059 and TPCK inhibit tumor progression in *rag2-KRAS^{G12D}*-induced zebrafish ERMS. (**A**) Scheme of the analysis strategy. Photographs of tumors were taken under standardized conditions at days 7, 10 and 13. Gray boxes indicate days of chemical or control treatment; white boxes represent recovery days. (**B-F**) Images of a representative tumor-bearing fish receiving vehicle control (DMSO) treatment. (B-D) Images of the tumor area with DsRed fluorescence labeling RAS activation at 7 (B), 10 (C) and 13 (D) dpf. Photographs were taken with an exposure time of 3 seconds and gain of 80%. (E) The overall length of each fish (nose to tail) was also recorded under brightfield illumination at 7, 10 and 13 dpf to ensure the general health of fish. (F) Overlay of B-D, demonstrating the relative growth of the tumor (red, 7 dpf; green, 10 dpf; yellow, 13 dpf). (**G**,**H**) Relative tumor growth in fish treated with (G) PD98059 (15.6 μM) or (H) TPCK (0.3 μM) compared with vehicle (DMSO or ethanol) treated siblings (P<0.05, ANOVA, chemical compared with vehicle treatment). Error bars indicate s.e.m.

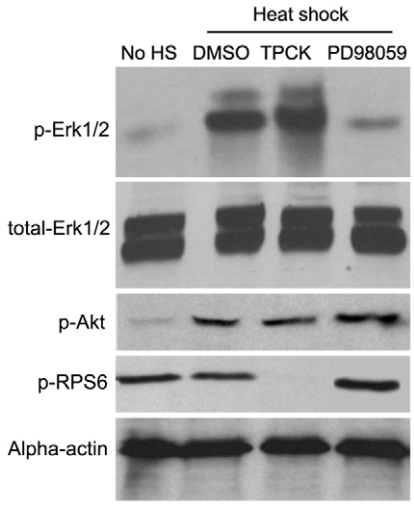

Fig. 4. PD98059 and TPCK selectively suppress different downstream RAS signaling pathways in zebrafish embryos. Western blot analysis was performed using *Tg(hsp70-HRAS^{G12V})* embryos to study the phosphorylation status of Erk1/2 (T202/Y204), Akt (S473) and Rps6 (S240). The embryos were treated with PD98059 (18.7 μM), TPCK (1 μM) or DMSO control from 22 hpf, heat shocked from 24-25 hpf at 37°C and whole embryos were homogenized in 1× SDS sample buffer at 28 hpf.

the S6K1 pathway without significantly suppressing the MAPK or AKT pathways in zebrafish.

To assess whether PD98059 and TPCK also have anti-tumor effects in human ERMS, each was assessed for growth and apoptotic effects in the human RD cell line that has activated RAS signaling through mutation of *NRAS* (*NRAS^{Q61H}*) (Stratton et al., 1989). By MTT assay in RD cells, both PD98059 (10 μM, 20 μM and 40 μM; $P<0.001$, ANOVA) and TPCK (1 μM, 5 μM and 10 μM; $P<0.001$, ANOVA) suppressed proliferation in a dose-dependent manner, with the greatest level of suppression seen at the highest dose (40 μM for PD98059 and 10 μM for TPCK; Fig. 5). By contrast, PD98059 showed no suppression of proliferation in mouse embryonic fibroblasts (MEFs) in a dose range of 10-60 μM ($P=0.68$, ANOVA; supplementary material Fig. S9A), with suppression only at a very high dose of 100 μM ($P<0.01$). TPCK showed no proliferation suppression at 0.3-30 μM ($P=0.75$, ANOVA; supplementary material Fig. S9B).

Apoptosis was measured in RD cells by TdT assay on day 4, but showed no increase in apoptosis in chemical-treated as compared with vehicle-treated cells (supplementary material Fig. S10). Thus, the main effect of PD98059 and TPCK is to suppress cell proliferation in the RAS-activated human rhabdomyosarcoma cell line, and this was unlikely to be through promoting apoptosis or toxicity. PD98059 and TPCK are bioactive in both zebrafish and human cells.

PD98059 and TPCK synergistically suppress tumor progression in zebrafish rhabdomyosarcoma and human RD cells

The above data indicate that PD98059 and TPCK act on independent signaling modules downstream of activated RAS; thus, we speculated that combined treatment with both compounds would result in an improved therapeutic effect. ERMS-bearing fish were treated with one-third of the MTD of each compound alone or in combination. A cohort of tumor-bearing fish was randomized into four groups at 7 dpf: (1) vehicle control [0.28% (v/v) DMSO], (2) PD98059 alone (5.2 μM), (3) TPCK alone (0.1 μM) and (4) PD98059 (5.2 μM) with TPCK (0.1 μM). Drug treatment, recovery and tumor measurement were carried out as described above. During the 6-day treatment regimen, single drug treatment at the lower concentration did not delay tumor progression (PD98059: 1.463±0.416, $n=13$; TPCK: 1.377±0.353, $n=7$; DMSO: 1.412±0.348, $n=12$; at day 10). Strikingly, combined treatment with TPCK and PD98059 achieved significant suppression of tumor growth compared with each single drug treatment or vehicle control (1.0697±0.221, $n=12$; $P=0.0009$, ANOVA; Fig. 6A,C). Overall fish growth was unaffected by drug treatment in all groups, suggesting that combined drug treatment elicited only anti-tumor effects on larval fish (supplementary material Fig. S7C). A similar synergistic anti-proliferative effect was observed in the human ERMS (RD) cell line when treated simultaneously with PD98059 and TPCK (Fig. 6B); however, drug combinations had no effect on apoptosis (supplementary material Fig. S10).

We have shown that TPCK suppresses the activity of S6K1. Because TPCK has been reported to have different effects on various signaling pathways, we next sought to demonstrate that TPCK treatment results in reduced proliferation through inhibition of the S6K pathway. Using lentivirus-mediated RNA interference, we tested whether knockdown of S6K1 could mimic the synergistic effect of TPCK on cell proliferation when combined with PD98059. An shRNA for S6K1 (shS6K1) was constructed and its effect confirmed in a cell proliferation assay. The suppressive effect of S6K1 knockdown combined with PD98059 (10 μM) or TPCK (2.5 μM) was compared with controls (scrambled shRNA) with either chemical alone or in combination (Fig. 6D). The relative growth of cells treated with shS6K1 and TPCK (1.582±0.074 at day 7, 1.663±0.05 at day 9) was not

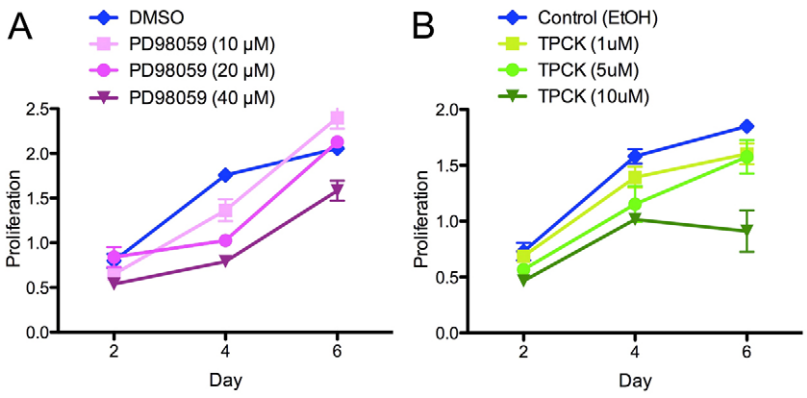

Fig. 5. PD98059 and TPCK suppress cell proliferation in the human RD cell line. Cells were plated in 96-well tissue culture plates at day −1. Cells were treated with a range of concentrations of (**A**) PD98059 (10-40 μM) or (**B**) TPCK (1-10 μM) starting at day 0 and continuing throughout the 6-day treatment. Medium/chemicals were changed on days 0, 2 and 4 to ensure chemical activity and adequate nutrients for cell growth. Cell proliferation was measured by MTT assay at days 2, 4 and 6. *y*-axis represents absolute OD from the MTT assay. Error bars indicate s.e.m.

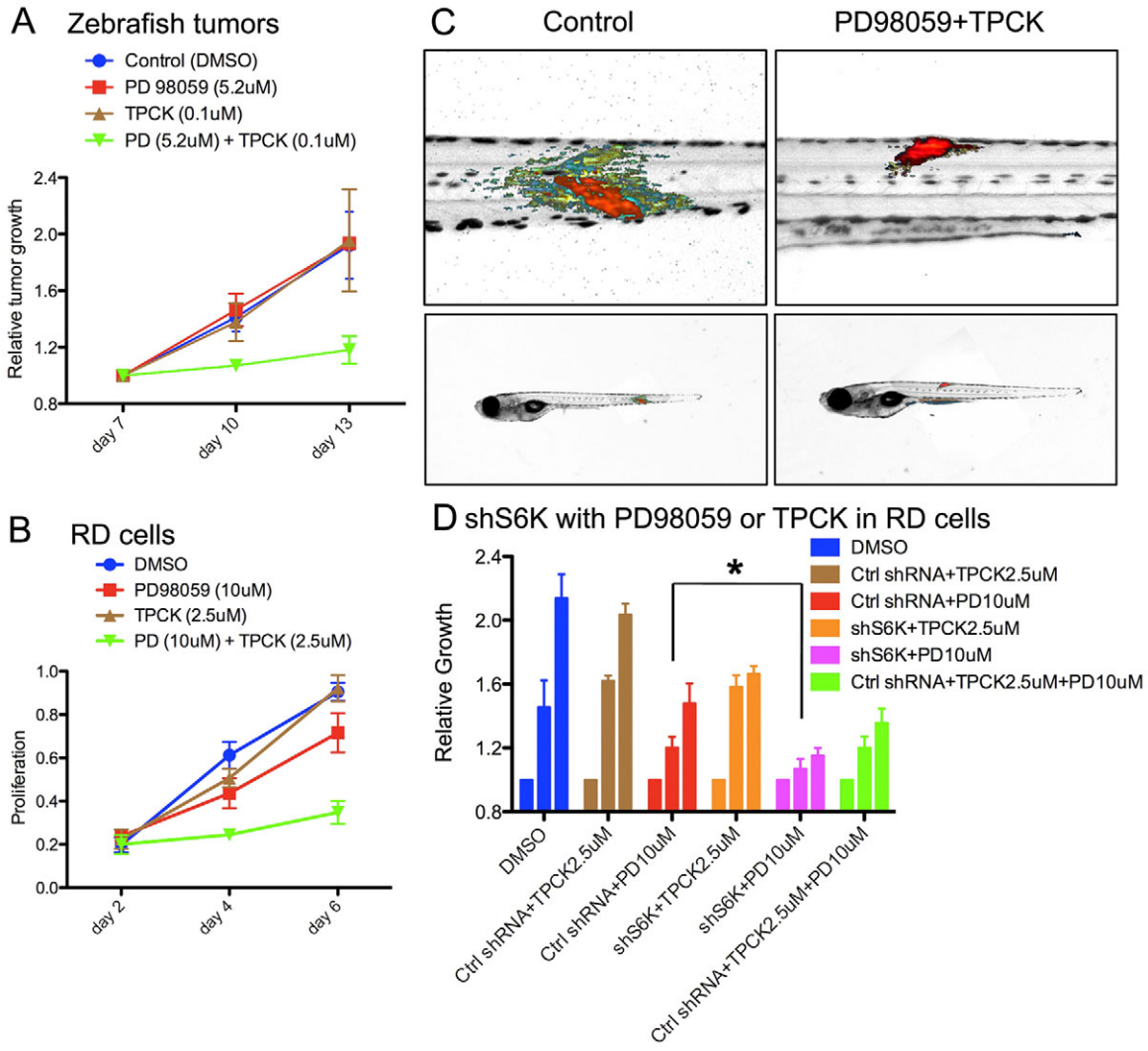

Fig. 6. PD98059 and TPCK synergistically suppress tumor progression in zebrafish ERMS and human RD cells. (**A**) Relative tumor growth in zebrafish ERMS with combination treatment (5.2 µM PD98059 + 0.1 µM TPCK, *n*=27), PD98059 (5.2 µM, *n*=13), TPCK (0.1 µM, *n*=7) and DMSO vehicle [0.28% (v/v), *n*=12]. *P*=0.009 (ANOVA, combined treatment compared with other conditoins) at day 10. (**B**) Human RD cell proliferation measured by MTT assay after vehicle [0.53% (v/v) DMSO], PD98059 (10 µM), TPCK (2.5 µM) or combination treatment (10 µM PD98059 + 2.5 µM TPCK). (**C**) Representative overlay images of zebrafish with *rag2-KRAS*^{G12D}-induced tumors treated with DMSO vehicle control and a combination of PD98059 and TPCK. Color code as in Fig. 3F. (**D**) RD cell proliferation measured by MTT assay after cells were treated with DMSO, control (scrambled) shRNA (Ctrl shRNA), S6K1 shRNA (shS6K1), TPCK (2.5 µM) and/or PD98059 (10 µM) as indicated. Three bars of the same color represent (left to right) relative cell growth under a given treatment condition on days 5, 7 and 9. *P<0.05 (ANOVA). Error bars indicate s.e.m.

significantly different from cells treated with TPCK alone (1.621±0.032 at day 7, 2.036±0.076 at day 9; *P*=0.13, ANOVA), suggesting that shS6K1 and TPCK are acting redundantly in the same pathway. By contrast, treatment with shS6K1 and PD98059 (1.069±0.063 at day 7, 1.151±0.048 at day 9) had a more potent suppressive effect compared with cells treated with PD98059 alone (1.202±0.067 at day 7, 1.479±0.125 at day 9; *P*=0.01, ANOVA), demonstrating a synergistic effect. This synergistic suppression by shS6K1 plus PD98059 was similar to that of TPCK plus PD98059 (1.201±0.070 at day 7, 1.357±0.089 at day 9; *P*=0.22, ANOVA). These data showed that S6K1 knockdown or pharmacological treatment with TPCK exhibited a similar synergistic effect when combined with PD98059, supporting the conclusion that TPCK suppresses cell proliferation through inhibiting the S6K1 pathway.

PD98059 and TPCK converge on translation initiation to suppress tumor proliferation

We next focused on understanding the mechanism of how TPCK and PD98059 synergistically suppress tumor cell growth. Studies from other groups suggest that the activated RAS/MAPK and AKT/S6K1 pathways both independently increase protein synthesis by optimizing cap-dependent translation initiation. An important component of this translation initiation complex is eukaryotic translation initiation factor 4B (eIF4B) (Gingras et al., 2001). A phosphorylation site at Ser422 of eIF4B was demonstrated to be partially responsive to mTOR/S6K1 and partially responsive to MEK/ERK/RSK (Holz et al., 2005; Shahbazian et al., 2006); thus, we hypothesized that dual inhibition of the MAPK and S6K1 pathways leads to complete suppression of eIF4B phosphorylation, whereas single pathway inhibition still allows eIF4B activation

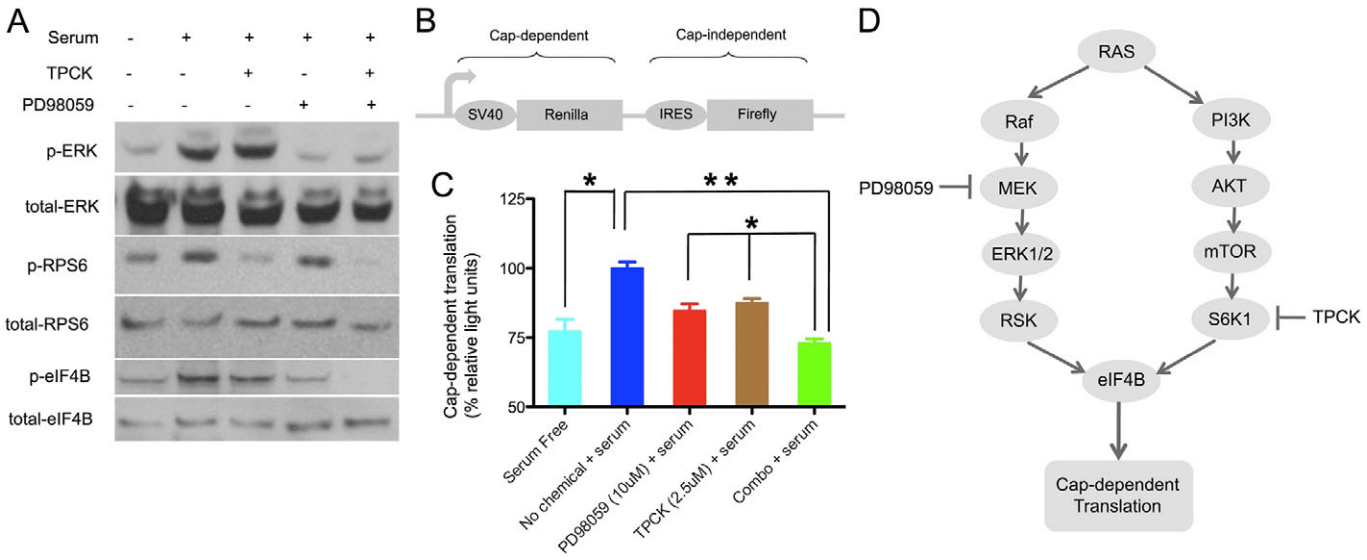

Fig. 7. The combination of PD98059 and TPCK suppresses eIF4B phosphorylation and cap-dependent translation initiation. (**A**) Human RD cells were deprived of serum overnight, treated with vehicle [0.53% (v/v) DMSO], PD98059 (10 μM), TPCK (2.5 μM) or a combination (10 μM PD98059 and 2.5 μM TPCK) for 2 hours, and then stimulated with serum (20%), or continued to be serum-starved, for 30 minutes. The phosphorylation status of ERK1/2 (T202/Y204), RPS6 (S235) and eIF4B (S422) was then analyzed by western blotting. (**B**) Structure of the bicistronic Renilla/firefly luciferase reporter plasmid used in the translation assay. (**C**) Cap-dependent translation in chemical-treated RD cells. RD cells were transfected with the reporter plasmid, after serum starvation for 12 hours, and then treated with control, PD98059, TPCK or a combination. Half an hour after chemical exposure, serum (20%) was added to cells to stimulate translation, luciferase activities were measured, and the Renilla/firefly luciferase light unit ratio was calculated. The value of the serum-stimulated sample was set at 100%. The experiment was performed in biological duplicate and technical triplicate. *P<0.05, **P<0.01 (Student's t-test). Error bars indicate s.e.m. (**D**) Proposed mechanism of suppression of translation initiation in tumor cells. MAPK/ERK and AKT/S6K1 are two major signaling pathways downstream of RAS. Blockage of both pathways results in effective suppression of eIF4B phosphorylation and inhibits translation initiation in proliferating tumor cells.

through the other pathway. Western blotting of eIF4B to detect phosphorylation of Ser422 was performed in RD cells treated with PD98059 and TPCK individually or in combination. As expected based on our zebrafish studies, p-ERK1/2 levels were suppressed by PD98059 and p-RPS6 levels were suppressed by TPCK; p-eIF4B levels were partially suppressed by PD98059 or TPCK single drug treatment, and were completely suppressed by combination treatment (Fig. 7A). These results suggest that PD98059 and TPCK synergistically downregulate the levels of p-eIF4B.

To demonstrate that suppression of p-eIF4B leads to suppression of cap-dependent translation activity, a bicistronic reporter was used to determine whether combined treatment with PD98059 and TPCK suppresses cap-dependent translation *in vivo*. This bicistronic luciferase reporter is structured so that the cap-dependent translation activity can be quantified relative to cap-independent translation (Fig. 7B) (Holz et al., 2005). The effects of single or combination treatments on cap-dependent translation were measured in comparison to vehicle-treated RD cells. Serum stimulation promoted cap-dependent translation (100±5.50%) compared with serum-starved cells (77.28±10.58%). Single chemical treatment resulted in a partial suppression of translation (Fig. 7C), whereas combined treatment in the presence of serum suppressed cap-dependent translation (72.91±4.68%; P<0.01 compared with the serum-stimulated level) to the serum-starved translation activity level. Taken together, these data indicate that PD98059 suppresses the MAPK pathway, whereas TPCK suppresses S6K1 activity, and each of these chemicals alone only partially affects eIF4B. Combined inhibition of the MAPK and S6K1 pathways results in diminished eIF4B phosphorylation and leads to potent suppression of translation initiation in tumor cells (Fig. 7D).

DISCUSSION

A common concept is that cancer cells often acquire embryonic character through activation of developmental pathways (Abbott et al., 2007; Dreesen and Brivanlou, 2007). Developmental biology has uncovered a number of signaling pathways involved in cancers; for example, the Hippo pathway was identified in *Drosophila* and shown to be crucial in cancer cell apoptosis (Saucedo and Edgar, 2007). Few studies have utilized zebrafish to directly compare the processes of embryogenesis and oncogenesis. Our work describes a new strategy to utilize zebrafish embryos to screen for pathways that participate in cancer development. We first demonstrated that conditional activation of oncogenic $HRAS^{G12V}$ in developing zebrafish embryos mimics RAS pathway activation during tumorigenesis. We then tested the therapeutic potential of these compounds on tumor progression in a zebrafish model of RAS-induced ERMS. This rhabdomyosarcoma model allows the study of tumors during larval development by 13 dpf, chemical exposure and direct imaging of tumors, demonstrating this tumor model as a powerful tool for cancer research. This two-step screening approach identified chemicals with anti-RAS activity that could be assessed in human cell lines that harbored *RAS* mutations, and identified pan-RAS inhibitors that modulate the function of all three RAS family members – $HRAS^{G12V}$ in our embryonic screen, $KRAS^{G12D}$ in zebrafish ERMS, and $NRAS^{Q61H}$ in the human RD cell line.

Among the hits in the screen, known inhibitors of both RAS activation and RAS downstream pathways were identified. For example, Lovastain is an inhibitor of 3-hydroxy-3-methylglutaryl-coenzyme A reductase (HMG-CoA reductase), a known inhibitor of RAS, and acts by suppressing the recruitment of RAS to the cell membrane (Issat et al., 2007). PD98059 was also identified in our

screen and is an inhibitor of MEK1, a major component of the MAPK cascade. The identification of these two groups of known inhibitors verified the design of our screen and demonstrated that the zebrafish embryo can be used to dissect specific signaling pathways *in vivo*.

TPCK was identified in our larval screen to suppress RAS pathway activation and also showed potent inhibition of ERMS growth as a single agent. TPCK was originally synthesized as a protease inhibitor (Schoellmann and Shaw, 1963). TPCK has been shown to be a potent *in vivo* inhibitor of S6K1, PDK1 and other related kinases with a conserved domain (known as AGC kinases), although an *in vitro* kinase assay showed that S6K1 is not the direct molecular target of TPCK (Ballif et al., 2001; Grammer and Blenis, 1996). TPCK has also been described as inhibiting the endoprotease responsible for cleaving the C-terminal AAX sequence on RAS (Porter et al., 2007). Alternative mechanisms have been proposed including recent work demonstrating that TPCK blocks specific cysteine residues on IkappaB kinase (IKK) and p65/RelA (Ha et al., 2009). TPCK was first found, 40 years ago, to potently inhibit tumorigenesis initiated in mouse skin lesions induced by DMBA (Troll et al., 1970), but the mechanism of how TPCK suppresses tumor growth remained unclear. In our experiments, TPCK completely abolished the RPS6 phosphorylation that is dependent on S6K1, without affecting p-ERK or p-AKT levels. Although α-actin was used as loading control for AKT and RPS6, our data from zebrafish embryos and cell culture argue against the possibility that TPCK inhibits the RAS CAAX modification as other RAS downstream pathways were relatively intact, but are instead consistent with the finding that TPCK is a suppressor of the S6K1 pathway. We further validated that both knockdown of S6K1 by lentivirus-mediated RNA interference and pharmacological treatment with TPCK demonstrated a similar synergistic effect with PD98059, suggesting that TPCK suppresses RD cell proliferation through inhibiting the S6K1 pathway. The toxicity of TPCK, however, has been a major concern (Lewis, 2004). To circumvent toxicity, we tested the efficacy of a combination treatment regimen using both PD98059 and TPCK at lower concentrations. PD98059 and TPCK delayed tumor progression individually but showed a greater effect in impeding tumor progression when the two were combined, even at a significantly lower dose.

Translational control in eukaryotic cells is crucial for gene regulation to rapidly adjust protein production in conditions of nutrient deprivation and stress (Sonenberg and Hinnebusch, 2009). Aberrant function of components of the translation machinery underlies a variety of human diseases including certain cancers and metabolic disorders. The MAPK and PI3K pathways regulate the translation machinery, especially at the translation initiation complex, which binds to the cap region of mRNA to initiate translation (Parsa and Holland, 2004). eIF4B plays a crucial role in recruiting the 40S ribosomal subunit to the mRNA (Ma and Blenis, 2009). In response to growth factors, eIF4B is phosphorylated on Ser422 by S6K1 and recruited to the translation initiation complex. When HeLa cells are stimulated with serum, a significant fraction of Ser422 phosphorylation remains resistant to inhibition by rapamycin. Further evidence indicates that the MEK/ERK target, p90 ribosomal protein S6 kinase (RSK), phosphorylates eIF4B on the same residue. Phosphorylation of eIF4B on Ser422 by both RSK and S6K increases the interaction of eIF4B with eIF3 (Holz et al., 2005; Shahbazian et al., 2006). The recruitment of the translation initiation complex increases the mRNA binding and processivity of the activated helicase complex, potentially enhancing translation rates. We showed that PD98059 or TPCK partially inhibits, whereas a combination of the two completely abolishes, eIF4B Ser422 phosphorylation. We further demonstrated that *in vivo* cap-dependent translation was significantly decreased after combination treatment, whereas it was only partially decreased by single agent treatments. We propose that the blockage of two major signaling pathways downstream of RAS – MAPK/ERK and AKT/S6K1 – results in effective suppression of eIF4B phosphorylation and the inhibition of translation initiation in proliferating tumor cells.

Our study interfaces embryogenesis and oncogenesis in a vertebrate model. We demonstrate successful use of zebrafish embryos and cancer models for anticancer chemical screens in a shared pathway, and proved the feasibility of performing chemical screens directly in tumor-bearing animals. By inhibiting both the MAPK/ERK and AKT/S6K1 pathways we showed that inhibition of translation initiation suppresses tumor growth, thereby demonstrating the translational initiation complex to be a drug target for cancer therapy.

Acknowledgements

We thank John Blenis for providing helpful advice and reagents; Xiaoying Bai, Richard White, Lili Jing and Christopher Salthouse for critical review of the manuscript; and Abby Barton for technical assistance.

Funding

L.I.Z. is supported by the National Institutes of Health [5 R01 CA103846-10] and Howard Hughes Medical Institute. D.M.L. is supported by the National Institutes of Health [K01AR05562190, R01CA154923, R21CA156056 and 1U54CA168512], The American Cancer Society, The Harvard Stem Cell Institute, The Sarcoma Foundation of America, and Alex Lemonade Stand Foundation. A.J.W. is supported by a Stand Up To Cancer-American Association for Cancer Research Innovative Research Grant [SU2C-AACR-IRG1111] and the National Institutes of Health [RO1 HL088582-01S1]. K.D.P. is supported by the National Institutes of Health [GM074057 and HL081674]. S.H. is supported by Hope Street Kids and P.A.L.S. Bermuda/St. Baldrick's. Deposited in PMC for release after 6 months.

Competing interests statement

L.I.Z. is a founder and stock holder of Fate, Inc. and a scientific advisor for Stemgent.

Supplementary material

Supplementary material available online at
http://dev.biologists.org/lookup/suppl/doi:10.1242/dev.088427/-/DC1

References

Abbott, D. E., Postovit, L.-M., Seftor, E. A., Margaryan, N. V., Seftor, R. E. B. and Hendrix, M. J. C. (2007). Exploiting the convergence of embryonic and tumorigenic signaling pathways to develop new therapeutic targets. *Stem Cell Rev.* **3**, 68-78.

Anjum, R. and Blenis, J. (2008). The RSK family of kinases: emerging roles in cellular signalling. *Nat. Rev. Mol. Cell Biol.* **9**, 747-758.

Ballif, B. A., Shimamura, A., Pae, E. and Blenis, J. (2001). Disruption of 3-phosphoinositide-dependent kinase 1 (PDK1) signaling by the anti-tumorigenic and anti-proliferative agent n-alpha-tosyl-l-phenylalanyl chloromethyl ketone. *J. Biol. Chem.* **276**, 12466-12475.

Bos, J. L. (1989). ras oncogenes in human cancer: a review. *Cancer Res.* **49**, 4682-4689.

Dovey, M., White, R. M. and Zon, L. I. (2009). Oncogenic NRAS cooperates with p53 loss to generate melanoma in zebrafish. *Zebrafish* **6**, 397-404.

Dreesen, O. and Brivanlou, A. H. (2007). Signaling pathways in cancer and embryonic stem cells. *Stem Cell Rev.* **3**, 7-17.

Easton, J. B. and Houghton, P. J. (2006). mTOR and cancer therapy. *Oncogene* **25**, 6436-6446.

Ekerot, M., Stavridis, M. P., Delavaine, L., Mitchell, M. P., Staples, C., Owens, D. M., Keenan, I. D., Dickinson, R. J., Storey, K. G. and Keyse, S. M. (2008). Negative-feedback regulation of FGF signalling by DUSP6/MKP-3 is driven by ERK1/2 and mediated by Ets factor binding to a conserved site within the DUSP6/MKP-3 gene promoter. *Biochem. J.* **412**, 287-298.

Gaiano, N., Amsterdam, A., Kawakami, K., Allende, M., Becker, T. and Hopkins, N. (1996). Insertional mutagenesis and rapid cloning of essential genes in zebrafish. *Nature* **383**, 829-832.

Gingras, A. C., Raught, B. and Sonenberg, N. (2001). Regulation of translation initiation by FRAP/mTOR. *Genes Dev.* **15**, 807-826.

Goessling, W., North, T. E. and Zon, L. I. (2007). New waves of discovery: modeling cancer in zebrafish. *J. Clin. Oncol.* **25**, 2473-2479.
Grammer, T. C. and Blenis, J. (1996). The serine protease inhibitors, tosylphenylalanine chloromethyl ketone and tosyllysine chloromethyl ketone, potently inhibit pp70s6k activation. *J. Biol. Chem.* **271**, 23650-23652.
Ha, K.-H., Byun, M.-S., Choi, J., Jeong, J., Lee, K.-J. and Jue, D.-M. (2009). N-tosyl-L-phenylalanine chloromethyl ketone inhibits NF-kappaB activation by blocking specific cysteine residues of IkappaB kinase beta and p65/RelA. *Biochemistry* **48**, 7271-7278.
Haffter, P., Granato, M., Brand, M., Mullins, M. C., Hammerschmidt, M., Kane, D. A., Odenthal, J., van Eeden, F. J., Jiang, Y. J., Heisenberg, C. P. et al. (1996). The identification of genes with unique and essential functions in the development of the zebrafish, Danio rerio. *Development* **123**, 1-36.
Holz, M. K., Ballif, B. A., Gygi, S. P. and Blenis, J. (2005). mTOR and S6K1 mediate assembly of the translation preinitiation complex through dynamic protein interchange and ordered phosphorylation events. *Cell* **123**, 569-580.
Issat, T., Nowis, D., Legat, M., Makowski, M., Klejman, M. P., Urbanski, J., Skierski, J., Koronkiewicz, M., Stoklosa, T., Brzezinska, A. et al. (2007). Potentiated antitumor effects of the combination treatment with statins and pamidronate in vitro and in vivo. *Int. J. Oncol.* **30**, 1413-1425.
Janknecht, R., Monté, D., Baert, J. L. and de Launoit, Y. (1996). The ETS-related transcription factor ERM is a nuclear target of signaling cascades involving MAPK and PKA. *Oncogene* **13**, 1745-1754.
Kawakami, Y., Rodríguez-León, J., Koth, C. M., Büscher, D., Itoh, T., Raya, A., Ng, J. K., Esteban, C. R., Takahashi, S., Henrique, D. et al. (2003). MKP3 mediates the cellular response to FGF8 signalling in the vertebrate limb. *Nat. Cell Biol.* **5**, 513-519.
Langenau, D. M., Keefe, M. D., Storer, N. Y., Guyon, J. R., Kutok, J. L., Le, X., Goessling, W., Neuberg, D. S., Kunkel, L. M. and Zon, L. I. (2007). Effects of RAS on the genesis of embryonal rhabdomyosarcoma. *Genes Dev.* **21**, 1382-1395.
Langenau, D. M., Keefe, M. D., Storer, N. Y., Jette, C. A., Smith, A. C. H., Ceol, C. J., Bourque, C., Look, A. T. and Zon, L. I. (2008). Co-injection strategies to modify radiation sensitivity and tumor initiation in transgenic Zebrafish. *Oncogene* **27**, 4242-4248.
Le, X., Langenau, D. M., Keefe, M. D., Kutok, J. L., Neuberg, D. S. and Zon, L. I. (2007). Heat shock-inducible Cre/Lox approaches to induce diverse types of tumors and hyperplasia in transgenic zebrafish. *Proc. Natl. Acad. Sci. USA* **104**, 9410-9415.
Lee, Y., Hami, D., De Val, S., Kagermeier-Schenk, B., Wills, A. A., Black, B. L., Weidinger, G. and Poss, K. D. (2009). Maintenance of blastemal proliferation by functionally diverse epidermis in regenerating zebrafish fins. *Dev. Biol.* **331**, 270-280.
Lewis, R. J., Sr (2004). *Sax's Dangerous Properties of Industrial Materials*, 11th edn, pp. 3497-3498. New York, USA: Wiley-Interscience.
Ma, X. M. and Blenis, J. (2009). Molecular mechanisms of mTOR-mediated translational control. *Nat. Rev. Mol. Cell Biol.* **10**, 307-318.
Malumbres, M. and Barbacid, M. (2003). RAS oncogenes: the first 30 years. *Nat. Rev. Cancer* **3**, 459-465.
McCubrey, J. A., Steelman, L. S., Chappell, W. H., Abrams, S. L., Wong, E. W. T., Chang, F., Lehmann, B., Terrian, D. M., Milella, M., Tafuri, A. et al. (2007). Roles of the Raf/MEK/ERK pathway in cell growth, malignant transformation and drug resistance. *Biochim. Biophys. Acta* **1773**, 1263-1284.
North, T. E., Goessling, W., Walkley, C. R., Lengerke, C., Kopani, K. R., Lord, A. M., Weber, G. J., Bowman, T. V., Jang, I.-H., Grosser, T. et al. (2007). Prostaglandin E2 regulates vertebrate haematopoietic stem cell homeostasis. *Nature* **447**, 1007-1011.
Parsa, A. T. and Holland, E. C. (2004). Cooperative translational control of gene expression by Ras and Akt in cancer. *Trends Mol. Med.* **10**, 607-613.
Porter, S. B., Hildebrandt, E. R., Breevoort, S. R., Mokry, D. Z., Dore, T. M. and Schmidt, W. K. (2007). Inhibition of the CaaX proteases Rce1p and Ste24p by peptidyl (acyloxy)methyl ketones. *Biochim. Biophys. Acta* **1773**, 853-862.
Pozios, K. C., Ding, J., Degger, B., Upton, Z. and Duan, C. (2001). IGFs stimulate zebrafish cell proliferation by activating MAP kinase and PI3-kinase-signaling pathways. *Am. J. Physiol.* **280**, R1230-R1239.
Rodriguez-Viciana, P., Warne, P. H., Dhand, R., Vanhaesebroeck, B., Gout, I., Fry, M. J., Waterfield, M. D. and Downward, J. (1994). Phosphatidylinositol-3-OH kinase as a direct target of Ras. *Nature* **370**, 527-532.
Roehl, H. and Nüsslein-Volhard, C. (2001). Zebrafish pea3 and erm are general targets of FGF8 signaling. *Curr. Biol.* **11**, 503-507.
Saucedo, L. J. and Edgar, B. A. (2007). Filling out the Hippo pathway. *Nat. Rev. Mol. Cell Biol.* **8**, 613-621.
Schier, A. F. (2001). Axis formation and patterning in zebrafish. *Curr. Opin. Genet. Dev.* **11**, 393-404.
Schoellmann, G. and Shaw, E. (1963). Direct evidence for the presence of histidine in the active center of chymotrypsin. *Biochemistry* **2**, 252-255.
Sebolt-Leopold, J. S., Dudley, D. T., Herrera, R., Van Becelaere, K., Wiland, A., Gowan, R. C., Tecle, H., Barrett, S. D., Bridges, A., Przybranowski, S. et al. (1999). Blockade of the MAP kinase pathway suppresses growth of colon tumors in vivo. *Nat. Med.* **5**, 810-816.
Shahbazian, D., Roux, P. P., Mieulet, V., Cohen, M. S., Raught, B., Taunton, J., Hershey, J. W. B., Blenis, J., Pende, M. and Sonenberg, N. (2006). The mTOR/PI3K and MAPK pathways converge on eIF4B to control its phosphorylation and activity. *EMBO J.* **25**, 2781-2791.
Sonenberg, N. and Hinnebusch, A. G. (2009). Regulation of translation initiation in eukaryotes: mechanisms and biological targets. *Cell* **136**, 731-745.
Stratton, M. R., Darling, J., Pilkington, G. J., Lantos, P. L., Reeves, B. R. and Cooper, C. S. (1989). Characterization of the human cell line TE671. *Carcinogenesis* **10**, 899-905.
Troll, W., Klassen, A. and Janoff, A. (1970). Tumorigenesis in mouse skin: inhibition by synthetic inhibitors of proteases. *Science* **169**, 1211-1213.